Effect of water on zinc (II), cadmium (II) complexes with pyridylimidazole: Theoretical study of stability and electronic spectrum

ARTICLE *in* INTERNATIONAL JOURNAL OF QUANTUM CHEMISTRY · FEBRUARY 2006

Impact Factor: 1.43 · DOI: 10.1002/qua.20756

6 AUTHORS, INCLUDING:

Yi Liao
Capital Normal University
44 PUBLICATIONS **829** CITATIONS
SEE PROFILE

Yu-He Kan
Huaiyin Normal University
137 PUBLICATIONS **1,049** CITATIONS
SEE PROFILE

Effect of Water on Zinc (II), Cadmium (II) Complexes With Pyridylimidazole: Theoretical Study of Stability and Electronic Spectrum

YI LIAO, ZHONG-MIN SU, YU-HE KAN, SHU-MEI YUE, JIAN-FANG MA, JI-HUA YANG

Institute of Functional Material Chemistry, Faculty of Chemistry, Northeast Normal University, Changchun 130024, People's Republic of China

Received 26 February 2005; accepted 27 May 2005
Published online 21 September 2005 in Wiley InterScience (www.interscience.wiley.com).
DOI 10.1002/qua.20756

ABSTRACT: The geometry structures of complexes such as $[Zn(PIm)_2(H_2O)]$ and $[Cd(PIm)_2(H_2O)_2]$ [PIm = (2-(2′-pyridyl) imidazole)] are optimized by density functional theory (DFT) B3LYP methods. On the basis of their stable structures, the stability of the coordinated water existing in the complexes is analyzed quantitatively in terms of the interaction between the central metal and the coordinated water. The interaction energy of the Zn pyridylimidazole complex increased obviously by considering the intermolecular hydrogen bond (O—H· · ·N). The theoretical calculation well explained penta- and hexa-coordinated conformation, respectively, in Zn and Cd pyridylimidazole complexes. The spectral properties of the Zn Cd complexes have been studied by time-dependent density functional theory (TD-DFT). The calculation results show that the coordinated waters in Cd complexes have little effect on their spectral properties. While the axially coordinated waters in Zn pyridylimidazole cause a red shift in the absorption wavelength and change the pattern of charge transfer as a result of the effect of polarization from intermolecular hydrogen bond. Int J Quantum Chem 106: 490–500, 2006

Key words: *ab initio*; time-dependent density functional theory; interaction energy; electronic spectrum; organometallic compound

Correspondence to: Z.-M. Su; e-mail: zmsu@nenu.edu.cn
Contract grant sponsor: National Natural Science Foundation of China.
Contract grant numbers: 20160025; 20243003.
This article contains supplementary material available via the Internet at http://www.interscience.wiley.com/jpages/0020-7608/suppmat.

Introduction

Organometallic compounds with imidazole play important roles in various biological processes and have been widely employed in drug design [1–4]. More recently, there is a rapidly growing interest in the study and design of metal complexes with imidazole derivatives due to the potential applications of these compounds in the field of electronic and optoelectronic devices such as field-effect transistors (FETs) and light-emitting diodes (LEDs) [5–7]. Several synthetic and spectral studies of metal benzimidazole and pyridylbenzimidazole complexes have been reported. For example, $Al(PBI)_3$ and $Be(PBI)_2$ (PBI; o-(*N*-phenyl-2-benzimidazolyl)phenol) with blue light emission were synthesized by Shi et al. [6]. Huang et al. [7] reported bright red electroluminescent devices using europium complexes with ligands 2-(2-pyridyl)benzimidazole (HPBM) and 1-ethyl-2-(2-pyridyl)benzimidazole (EPBM) as the emitting layer. Our group systematically synthesized blue light-emitting pyridylbenzimidazole complexes of Cd(II) and Zn(II) [8], hereinafter abbreviated as $Zn(PBIm)_2$ and $Cd(PBIm)_2$. Crystal waters can often be found in these luminescent Zn, Cd pyridylbenzimidazole complexes. Stable Zn complexes adopt penta-coordinated and Cd complexes prefer hexa-coordinated (see Supporting Information).

The coordination numbers of the metal ions of the first transition series are usually four or six [9]. Penta-coordinated species are seldom recognized for ions such as zinc [10–13], and there is no report revealing the reasons responsible for this configuration. It is known that the photophysical properties of complexes are closely related to their structural features; therefore, it is important to investigate the stable coordinate structures of these Zn, Cd pyridylimidazole complexes.

To be used as an efficient electroluminescent material, an organometallic compound should be highly photoluminescent. It has long been recognized that the water molecule can result in low photoluminescent quantum efficiency by quenching the luminescence of complexes through nonradiative exchange of the exciton energy to the high vibration modes of OH-groups [14, 15]. Research efforts into the effect of coordinated water on luminescence have been carried out in the areas of experimental measurements. To the best of our knowledge, no theoretical calculations have been carried out to explore this issue. But it may be a difficult subject to fully understand the luminescent mechanism of these complexes with coordinated water unless we can discuss them in detail at an electronic structural level, i.e., analyze them in terms of the nature of the excited state and the interactions between the orbitals of the metal and orbitals of coordinated water. Theoretical studies can offer the most important information on these aspects.

In the present study, we perform a systematic theoretical study on the stable structures, interaction energies, and low-lying excited states of series of Zn(II) and Cd(II) pyridylimidazole complexes, using density functional theory (DFT) methods. The stability of the coordinated water and its influence on electronic structure and spectral properties of these complexes are investigated.

Calculation Methods

The Gaussian 03 program [16] was used for quantum chemistry calculations. All geometries were fully optimized using DFT with Becke's three-parameter hybrid exchange potential (B3) [17] and the Lee–Yang–Parr (LYP) [18] correlation functional without symmetry constraints. Frequency calculations at the same level of theory have also been performed to identify all stationary points as minima (zero imaginary frequency). Recent studies show that DFT calculations are remarkably successful in predicting a wide variety of problems in organometallic chemistry [19–22]. Two kinds of basis set systems were used. The smaller one, denoted BS-1, is the split-valence 6-31G* basis set [23] for all atoms except Cd, where core electrons were replaced with the effective core potentials (ECPs), and its valence electrons were represented with a (21/21/31) set [24]. The larger one (BS-2) adopts same ECPs and the associated double-ζ basis set on Cd augmented with an *f*-polarization function. For other elements, the 6-31G basis set is used with polarization and diffusion functions. The gradient optimizations, frequency calculations, and evaluation of excitation energies were carried out using the BS-1 basis set, while the total energies for account of interaction energy were obtained by single-point calculations with the BS-2 basis set.

To carry out theoretical studies on the stable regularity of the coordinated waters that exist in the complexes, the interaction energies between metal ions M^{2+} and waters were calculated, and the basis set superposition error (BSSE) [25] was corrected by

the counterpoise method proposed by Boys and Bernardi [26]. The interaction energy is defined as the difference between the energy of the complex and the energies of the component molecules in which all the orbitals of the "ghost" system are included.

Vertical excitation energies were evaluated on optimized ground-state geometries with Gaussian implementation of time-dependent density functional theory (TD-DFT) [27]. TD-DFT in combination with B3LYP has proved a reliable approach for the theoretical treatment of electronic excitation processes [28–31]; recent work demonstrates the good accuracy for a wide range of organometallic systems [32–36]. Charmant et al. [33] successfully applied TD-B3LYP in studying the first excited-state features of platinum–thallium (Pt–Tl) alkynyl complexes, from which the luminescence is attributed to charge transfer from the Pt–Tl unit to the platinum metal fragments. Halls and Schlegel [34] and Martin et al. [35] have studied the lowest singlet excited states of tris(8-hydroxyquinolate)aluminum (Alq3) with the TD-B3LYP approach, and the calculated excitation and emission energies were in excellent agreement with the experimental values. Han and Lee [36] also reported from their systematic calculations on methyl-substituted tris(8-hydroxyquinolate)aluminum (Almq3) that the TD-B3LYP method provided the most reliable results for the transition energies. All calculations described in this study were performed at the SGI Origin 2000 server.

Results and Discussion

For computational ease, Zn(II) and Cd(II) pyridylimidazole complexes ($Zn(PIm)_2$, $Cd(PIm)_2$) were used as the models for $Zn(PBIm)_2$ and $Cd(PBIm)_2$ based on respective crystal structures, where pyridylbenzimidazole was substituted for pyridylimidazole. The general technique of employing hydrogen to substitute for phenyl, methyl, and so on, is useful in conserving computational resources.

The original structures of complexes ($[Zn(PIm)_2(H_2O)]$ (**1**) and $[Cd(PIm)_2(H_2O)_2]$ (**2**) are adopted from the crystal data [8]. To tail the influence of the coordinated water on the spectral properties, the nonwater systems corresponding to **1–2** (i.e., **3–4**), are presented as $[Zn(PIm)_2]$ (**3**) and $[Cd(PIm)_2]$ (**4**). Two-water systems of Zn^{2+} complexes, $[Zn(PIm)_2(H_2O)_2]$ (**5**), $[Zn(PIm)_2(H_2O)] \cdot H_2O$ (**6**), and dimeric system $[Zn(PIm)_2(H_2O)]_2$ (**7**) (see Fig. 1) are also studied for discussing the stability of coordinated water.

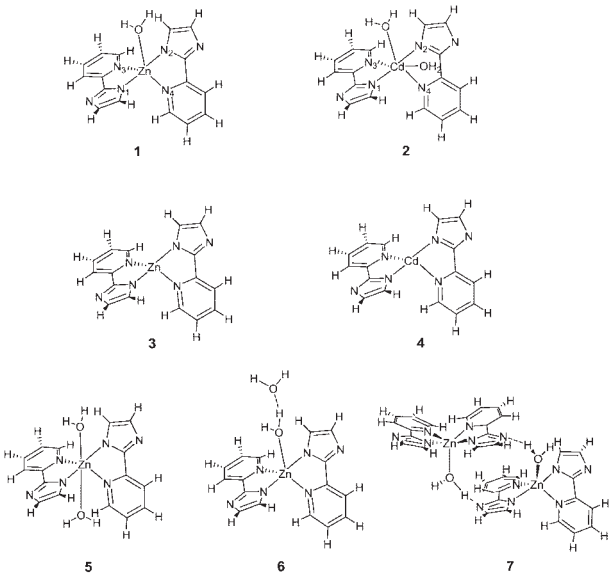

FIGURE 1. Schematic structures of systems **1–7** (labeled to help in reading Table I).

STABLE STRUCTURES OF THE COMPLEXES

The results of the optimized structures from B3LYP/BS-1 for systems **1–7** are summarized in Table I and shown in Figure 1.

The two idealized geometries of the fifth coordination are the trigonal bipyramid and the square pyramid. Our optimized structure of penta-coordinated system **1** can be described as a distorted trigonal bipyramid with two imidazole N atoms at the apical position (N1—Zn—N2═174°) and O, N3, N4 on the basal plane (N3—Zn—N4═121.9°, N3—Zn—O═121.7°, N4—Zn—O═116.3°). Hoskins and Whillans [37] pointed out in their review that the trigonal bipyramidal geometry might prove to be the most common ground state in the absence of ligand field stabilization. Since Zn^{2+} has a filled *d*-shell and is not subject to ligand field effects, the trigonal bipyramidal configuration is favored over the square pyramidal conformation, as confirmed by our X-ray diffraction [8].

In comparing the stable structure of system **1** with system **3,** we can see that such a penta-coordinated Zn pyridylimidazole complex is related to the much smaller bite angle between 2-(2′-pyridyl) imidazole and Zn (N1—Zn—N3: 84.5° in systems **3**) than to the standard tetrahedral coordination angle

TABLE I

Calculated geometrical parameters for systems 1–7 and vibrational frequencies (cm^{-1}) for O—H bond with B3LYP/BS-1.*

	Zn—N_1	Zn—N_3	N_1—Zn—N_3	Zn—O	O—H	V_{OH} str.	V_{OH} sci.	V_{OH} wag
$[Zn(PIm)_2(H_2O)]$ (**1**)	2.02	2.11	81.6	2.20	0.97	3849	1638	530
$[Cd(PIm)_2(H_2O)_2]$ (**2**)	2.29	2.42	73.6	2.46	0.97	3795	1708	530
$[Zn(PIm)_2]$ (**3**)	1.95	2.07	84.5	—	—	—	—	—
$[Cd(PIm)_2]$ (**4**)	2.20	2.36	76.3	—	—	—	—	—
$[Zn(PIm)_2(H_2O)]_2$ (**7**)	2.06	2.12	81.0	2.06	1.02	2080	1678	610

* All bonds are in Å and all angles are in deg.

(109.5°), which leads to unoccupied coordination space left for some small ligands such as H_2O. A similar situation has been found in the Zn complex of 2-(2′-pyridyl)indole ($Zn(2\text{-py-in})_2THF$), where Zn is penta-coordinated and the fifth coordinate site is occupied by an oxygen atom from solvent molecule tetrahydrofuran (THF) [13].

One may ask whether the unoccupied coordination space around Zn is large enough for further binding another H_2O to Zn^{2+}. To provide insight into the stable conformation of hydrated Zn pyridylimidazole complex, optimization of the hexa-coordinated system $[Zn(PIm)_2(H_2O)_2]$ (**5**) is carried out. Energy minimization shows that structure 5, where the two water molecules lie on the opposite side of Zn^{2+}, is only a local minimum on the potential energy surface. This is due to the steric strain in the complex. Hexa-coordinated system **5** has a penta-coordinated isomer $[Zn(PIm)_2(H_2O)] \cdot H_2O$ (**6**), in which the outer water connects with the inner coordinated water through intermolecular hydrogen bond (H—O…H) (Fig. 1). The ab initio calculation at the B3LYP/6-31G* level reveals that system **6** is $\geq$57.22 $kJ \cdot mol^{-1}$ lower in energy than system **5.** This demonstrates that zinc ions coordinated by the deprotonated pyridylimidazole prefer not a hexa-coordinated but a penta-coordinated environment involving one water molecule. Contrarily, in the case of system $[Cd(PIm)_2(H_2O)_2]$ (**2**), the two waters lie on the same side of Cd^{2+} (O—Cd—O: 86.5°). The optimal binding geometry for a divalent Cd coordinated by the pyridylimdazole ligands is hexa-coordinated involving two water molecules. This can be rationalized by the fact that the larger Pauling radius of Cd^{2+} (0.97 Å) relative to Zn^{2+} (0.74 Å) makes steric repulsion less important.

It should be pointed out that most geometric parameters calculated for systems **1** and **2** are in good agreement with the experimental data, and the deviations are $<$0.04 Å, except that the calculated Zn—O bond length (2.20 Å) is 0.2 Å longer than the measured value. This difference is larger, however, than would be expected from insufficient corrections for electron correlation and relativistic effects. One possible reason for this difference is the influence of intermolecular interaction that exists in the practical crystal, which is ignored in monomolecule calculation. X-ray diffraction study shows that between neighboring $[Zn(PIm)_2(H_2O)]$ molecules there are two intermolecular hydrogen bonds of the axially coordinated water molecules with the N atoms of the neighbor deprotonated imidazoles (see Supporting Information). We believe that the presence of the intermolecular hydrogen bonds may polarize the coordinated water molecule and shorten Zn—O bond. Therefore, system **1** is re-optimized in its dimer form (system **7**). The resulting Zn—O bond length is 2.06 Å, consistent with experimental observation. Recently, a similar observation was obtained by Åkesson et al. [38]. In their study, experimental M—O (H_2O) bond lengths are often found to be shorter than those calculated because the second coordination sphere hydrogen bound to water can polarize the water molecules and shorten the M—O bonds.

To gain further insight into this intermolecular hydrogen bond, a harmonic force field was calculated at the B3LYP/BS1 level of theory (see Table I). We can see from Table I that the OH stretching mode shifts from 3849 cm^{-1} (monomer **1**) to 2080 cm^{-1} (dimer 7). This is consistent with the weakening of the OH bond in system **7** (bond length increase from 0.97 to 1.02 Å) as a result of strong intermolecular hydrogen bonding. In contrast, the scissoring and wagging modes for OH undergo minor blue shifts from the monomer to the dimer system. More specifically, the OH scissoring fre-

TABLE II

Interaction energies (kJ · mol) between metal and water at B3LYP/BS-2 level.*

	System **1**	System **7**	System **2**
ΔE	−36.42	−60.35	−50.61
ΔE^B	−25.64	−51.12	−42.28

* ΔE^B, ΔE denoted as corrected and uncorrected interaction energy, respectively.

quency increases from 1638 cm^{-1} (monomer **1**) to 1678 cm^{-1} (dimer 7). Similarly, the OH wagging frequency increases from 530 cm^{-1} (monomer **1**) to 610 cm^{-1} (dimer 7). Again, all these effects suggest the presence of strong hydrogen bonding. Both scissoring and wagging motions for OH become hindered as a result of hydrogen bonding, increasing the scissoring and wagging force constants. It turns out from the above discussion that the high vibration modes of OH groups decrease significantly and the low vibration modes increase only slightly due to intermolecular hydrogen bonds, which may partially account for the high luminescent quantum efficiency in hydrated Zn pyridylimidazole.

We can see from Figure 1 that atom O (H_2O) coordinates with Zn^{2+} nearly along the C_2 axis for each dimer unit. This axially coordinated water molecule would be expected to have a strong influence on the geometric and electronic structure of the complex, and thus its photophysical properties. As shown in Table I, the main parameters of each stationary point vary significantly in going from nonwater systems to hydrated systems. For example, Zn—N bond lengths, especially of Zn-imidazole N, increase from 1.95 Å (**3**) to 2.06 Å (**7**). This indicates that binding between metal ion and pyridylimidazole ligand becomes weakened when water is axially coordinated to a metal center. In the following section, the interaction of M—H_2O will be investigated quantitatively.

INTERACTION ENERGIES OF M—O

The uncorrected interaction energies (ΔE) and CP corrected interaction energies (ΔE^B) by means of B3LYP/BS-2 are shown in Table II. BSSE = ΔE^B–ΔE reflects the effect of the basis set on interaction energy of M—O (metal segment–H_2O). It can be seen that the BSSEs of all systems range from 8 to 11 kJ · mol, accounting for 18–42% of the interaction energies. Therefore, BSSE should be taken into consideration.

As shown in Table II, ΔE^B of Zn–H_2O increases from 25.64 kJ · mol^{-1} (system **1**) to 51.12 kJ · mol^{-1} (system **7**) when the intermolecular hydrogen-bonding interaction is taken into account in a penta-coordinated system. This result explains rationally that the experimental existence of the penta-coordinated Zn–water complexes with deprotonated pyridylimidazole can be ascribed to the effect of polarization with intermolecular hydrogen bonds.

As in the case of same group element Cd^{2+}, since the ionic radius is comparatively large and the Cd^{2+} is more polarizable than borderline metal ion Zn^{2+} according to hard and soft acids and bases (HSAB) [39, 40], the M–H_2O interaction energy of hexa-coordinated system **2** is observed to be 42.28 kJ · mol^{-1}, indicative of a stable hexa-coordinated Cd pyridylimidazole complex.

FRONTIER MOLECULAR ORBITAL ANALYSIS

It will be useful to examine the frontier molecular orbitals (FMO) of system $[Zn(PIm)_2(H_2O)]_2$ (**7**) and $[Cd(PIm)_2(H_2O)_2]$ (**2**) to gain deeper insight into the effect of coordinate water and provide the framework for the excited-state TD-DFT calculations in the subsequent section.

Figure 2 plots the highest occupied orbitals (HOMO) and the lowest unoccupied orbitals (LUMO) of system $[Cd(PIm)_2(H_2O)_2]$ (**2**) and $[Cd(PIm)_2$ (**4**). FMOs of system $[Zn(PIm)_2]$ (**3**) and $[Zn(PIm)_2(H_2O)]_2$ (**7**) are illustrated in Figure 3. For clarity, some FMO compositions have also been analyzed (shown in Tables III and IV).

We can see from Figure 2 and Table III that the coordinated waters have little effect on FMOs of system **2** and only slightly altered the equally distributed orbital population on both PIm ligands (A and B). The FMOs are nearly identical for both Cd systems, in terms of their contributions (i.e., coefficients and phase) from the ligand-based atomic orbitals. The HOMO and HOMO-1 are near-degenerate. Likewise, the LUMO and LUMO-1 are also near degenerate. The HOMOs for both systems consist of the atomic orbitals of both imidazole and pyridyl rings with a dominant imidazole contribution (~76%). The LUMOs comprise mainly atomic orbitals of the pyridyl ring (~83%), accompanying little contribution from *d*-orbital of metal center. Thus similar spectrum properties are expected for system **2** and **4,** as proved by our spectral calculation later.

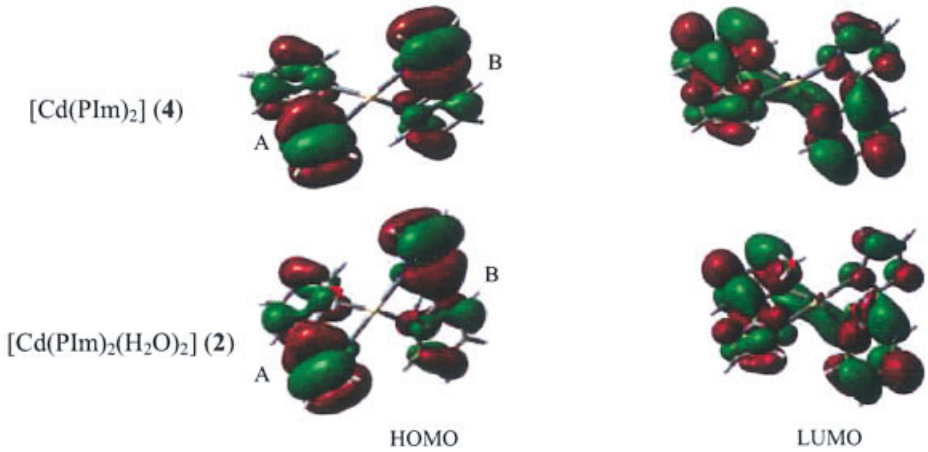

FIGURE 2. Plots of the frontier molecular orbitals of system $[Cd(PIm)_2(H_2O)_2]$ (**2**) and $[Cd(PIm)_2]$ (**4**). [Color figure can be viewed in the online issue, which is available at www.interscience.wiley.com.]

In a similar way, HOMO, HOMO-1, HOMO-2, LUMO, LUMO+1, and LUMO+2 are all π-type orbitals of the PIm ligand for both Zn complexes (**3** and **7**). The HOMOs are mainly centered on imidazole ring (about 76%); the LUMOs are π^* orbitals and consist mostly of atomic orbitals (about 84%) from the pyridyl ring. As one may see, there are few components of metal and water in FMOs (Fig. 3 and Table IV). The main bonding of a water to a transition metal center is well established and best described in terms of overlap of the p-orbital of the atom O with a metal fragment orbital of similar symmetry. Here interaction between the $3d$, $4s$ hybridized orbital of Zn and O p_z-orbital forming stable Zn—O σ bond was found in lower orbitals 161 and 162. They will not participate in low-lying optical excitation due to their low energy level.

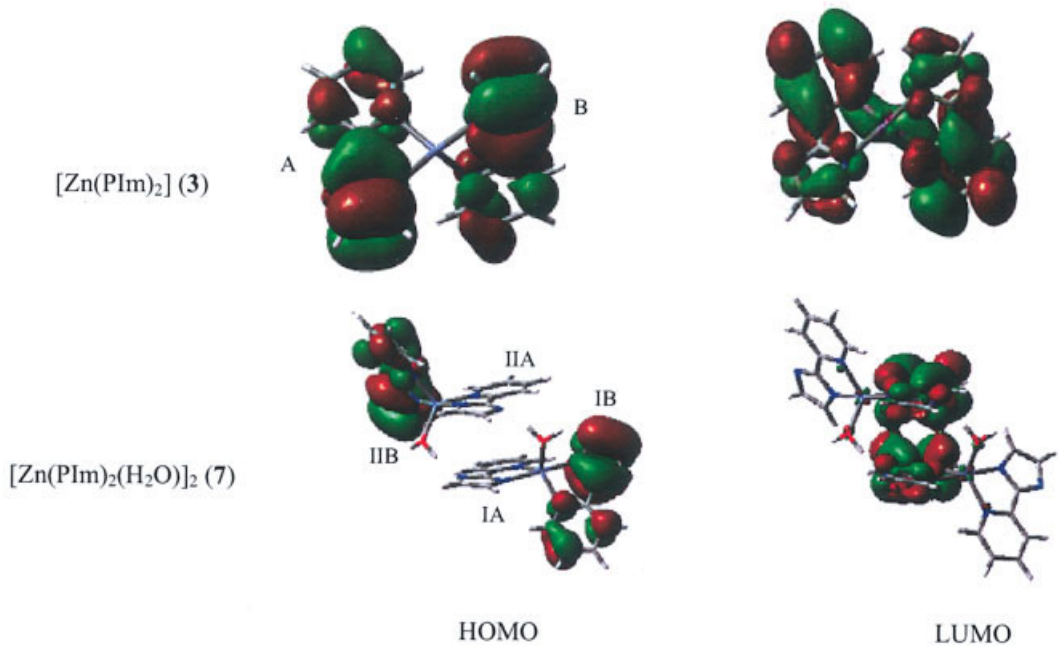

FIGURE 3. Plots of the frontier molecular orbitals of system $[Zn(PIm)_2]$ (**3**) and $[Zn(PIm)_2(H_2O)]_2$ (**7**). [Color figure can be viewed in the online issue, which is available at www.interscience.wiley.com.]

TABLE III

Calculated highest occupied and lowest virtual orbitals with character for the two Cd complexes.

Orbital	Energy (eV)	Composition % Cd	H_2O	Imidazole rings A	Imidazole rings B	Pyridyl ring A	Pyridyl ring B	Character
				$[Cd(PIm)_2(H_2O)_2]$ (**2**)				
Virtual								
94	−0.8515	1.3	0.1	3.8	3.8	45.6	45.4	π^*(Pyridyl)
93	−1.4602	1.1	1.3	7.7	7.7	41.1	41.1	π^*(Pyridyl)
92	−1.4781	1.0	1.8	7.3	7.3	41.3	41.3	π^*(Pyridyl)
Occupied								
91	−5.3784	0.1	0.0	39.6	36.8	12.2	11.3	π(Imidazole)
90	−5.3784	2.2	1.1	40.7	41.0	7.5	7.5	π(Imidazole)
89	−6.8356	0.8	0.5	44.4	44.2	5.1	5.1	π(Imidazole)
				$[Cd(PIm)_2]$ (**4**)				
Virtual								
85	−0.6321	0.3		4.2	4.2	45.6	45.6	π^*(Pyridyl)
84	−0.6678	0.2		4.25	4.3	45.6	45.6	π^*(Pyridyl)
83	−1.1644	2.1		7.4	7.4	41.5	41.5	π^*(Pyridyl)
82	−1.2338	2.5		7.51	7.5	41.3	41.3	π^*(Pyridyl)
Occupied								
81	−5.2293	0.1		38.2	38.2	11.8	11.8	π(Imidazole)
80	−5.2350	0.0		38.2	38.2	11.8	11.8	π(Imidazole)
79	−6.6459	1.2		44.6	44.6	4.8	4.8	π(Imidazole)

It should be emphasized that the axially coordinate water in system **7** has great impact on its FMO. In system **7,** the electron atmosphere of FMOs localizes mainly on the single PIm ligand (A or B) (see Fig. 3 and Table IV) instead of equal distribution on both ligands (A and B), as the case in system **3.** This is likely a result of the intermolecular hydrogen bonds of the coordinated water with the neighboring molecules and the π–π interactions between the pairs of the parallel PIm ligands. As a consequence, the first optically allowed excitation of system **7,** corresponding essentially to an HOMO–LUMO transition (see next section), would be different from system **3.**

EXCITATION ENERGIES

Ten singlet and triplet excited states are produced by the TD routine of DFT in the energy ranges of the absorption spectra for system **2, 3,** and **4,** and twice as many excited states are obtained for dimer system **7** based on their ground-state geometries, respectively. Contrary to the classical treatment of vertical one-electron excitation, the excited states calculated through TDDFT are described in terms of combinations of several transitions from occupied to virtual molecular orbitals.

Only the lowest triplet excited states (T_1) and the singlet excited states with maximum absorption wavelength and maximum oscillator strengths are listed in Table V.

The lowest spin-allowed transition ($S_0 \rightarrow S_1$) for system $[Cd(PIm)_2(H_2O)_2]$ (**2**) and $[Cd(PIm)_2$ (**4**) at the DFT level of theory is mainly transition HOMO → LUMO in character, which corresponds to an electronic excitation from the π-orbitals of imdazole ring into π^*-orbitals localized predominantly on the pyridyl ring (IL), mixing with little ligand-to-metal charge transfer (LMCT) (see Fig. 2 and Table V). The intense singlet absorption bands are observed at a relative higher-energy region (4.1–4.13 eV), which also corresponds to $\pi\pi^*$ (IL) excitation. We can observe similar singlet excited states between systems **2** and **4** because the coordinate waters of the Cd pyridylimidazole system have little influence on its FMOs.

The ultraviolet (UV) absorption spectra at room temperature, as well as our theoretical calculations, show that the excited states of Zn, Cd pyridylimidazole are dominated by a singlet–singlet transition

TABLE IV

Calculated highest occupied and lowest virtual orbitals with character for the two Zn complexes.

Orbital	Energy (eV)	Composition %										Character
				Imidazole rings				Pyridyl ring				
		Zn	H_2O	IA	IB	IIA	IIB	IA	IB	IIA	IIB	
						$[Zn(PIm)_2(H_2O)]_2$ (**7**)						
Virtual												
193	−1.2019	1.1	0.3	0.1	6.6	0.1	6.6	1.2	41.5	1.2	41.4	π^*(Pyridyl)
192	−1.5679	1.4	1.0	10.2	0.9	10.2	0.9	36.4	1.3	36.3	1.3	π^*(Pyridyl)
191	−1.5897	1.7	0.6	4.8	0.5	4.8	0.5	42.8	0.7	42.9	0.7	π^*(Pyridyl)
Occupied												
190	−5.3152	0.1	0.1	0.0	37.5	0.0	38.0	0.3	11.7	0.3	11.9	π^*(Imidazole)
189	−5.3155	0.1	0.1	0.0	38.0	0.0	37.5	0.4	11.9	0.4	11.7	π(Imidazole)
188	−5.5193	0.1	0.1	38.6	0.0	38.6	0.0	11.0	0.2	11.0	0.2	π(Imidazole)
162	−9.7785	14.5	26.4	7.2	3.0	7.2	3.0	13.9	5.4	13.9	5.4	σ(Zn, O, pyridyl)
161	−9.7948	14.8	31.4	3.7	4.3	3.7	4.3	13.9	5.0	13.9	5.0	σ(Zn, O, pyridyl)
						$[Zn(PIm)_2]$ (**3**)						
Virtual												
98	−0.9241	0.2		4.8	4.8			45.1	45.1			π^*(Pyridyl)
97	−1.5641	1.6		7.1	7.1			42	42			π^*(Pyridyl)
96	−1.5889	1.9		6.9	6.9			42.1	42.1			π^*(Pyridyl)
Occupied												
95	−5.4238	0.0		38.1	38.1			11.7	11.7			π(Imidazole)
94	−5.4241	0.3		38	38			11.8	11.8			π(Imidazole)
93	−6.8611	2.8		45.1	45.1			3.4	3.4			π(Imidazole)

of $\pi\pi^*$ character (see Supporting Information). However, the triplet excited state should also be taken into consideration due to the low temperature and heavy atom have evident influence on phosphorescence. Heavy metal complexes, particularly those containing 4*d* or 5*d* electrons, may have strong electron spin and orbital motions coupling [41]. The consequence of this spin-orbit coupling is mixing of electronic states with different multiplicity, which facilitates intersystem crossing from the singlet to triplet state, thus allowing the latter to acquire intensity in both absorption and emission. The TD-DFT results do not provide information on triplet–singlet absorption intensities since spin-orbit coupling effects are not included in current TD-DFT approaches, which is why the oscillator strengths are all zero for our calculated triplet excited states. However, the TD-DFT results should still provide a reasonable description of the overall orbital excitations that would be coupled in a subsequent spin-orbit treatment.

Transitions to the triplet states tend to be lower in energy than their corresponding singlets. For example, system **2,** the first triplet vertical transition energy, is 0.87 eV lower than that of the first singlet excited state (3.53 eV), where both represent (predominantly) a HOMO → LUMO transition.

The $S_0 \rightarrow S_1$ vertical transition energy of $[Cd(PIm)_2(H_2O)_2]$ calculated with the TD-DFT method predicts an absorption at 351 nm, which compares favorably with the experimental value of 350 nm in the solid state (see Supporting Information). Therefore, TD-DFT with a B3LYP functional can give relatively accurate predictions on vertical excitation energies for this series of systems.

Low-lying singlet excited states of $[Zn(PIm)_2]$ (**3**) and $[Zn(PIm)_2(H_2O)]_2$ (**7**) have also been studied by TD-DFT using a hybrid functional of B3LYP with 6-31G* basis set. The lowest energy excitation of $[Zn(PIm)_2(H_2O)]_2$ (**7**) is calculated at a 386-nm, 15-nm red shift relative to that of $[Zn(PIm)_2]$ (**3**). The intermolecular hydrogen-bonding interaction in system **7** is clearly responsible for the decrease of bandgap, and thus the red shift of the lowest absorption energy. In a similar way, the absorption peak at 310 nm in system **7** is also red shift as compared with that of system **3** (302 nm).

TABLE V

Selected calculated excitation energies (*E*), wavelengths (λ), oscillator strengths (*f*), and dominant excitation character for low-lying singlet (S_n) states and the lowest triplet excited states (T_1) of model systems.*

Systems	State	Composition		Nature	ΔE (eV)/λ (nm)	*f*	Character
	S_1	H → L	65%	$\pi \rightarrow \pi^*$	3.44/360	0.03	IL/LMCT
$[Cd(PIm)_2]$	S_7	H−1 → L+3	55%	$\pi \rightarrow \pi^*$	4.09/303	0.26	IL/LMCT
(**4**)	T_1	H → L	51%				
		H−1 → L+1	50%	$\pi \rightarrow \pi^*$	2.59/478	0.00	IL/LMCT
	S_1	H → L	67%	$\pi \rightarrow \pi^*$	3.53/351	0.03	IL/LMCT
$[Cd(PIm)_2(H_2O)_2]$	S_8	H → L+2	50%	$\pi \rightarrow \pi^*$	4.13/300	0.36	IL/LMCT
(**2**)	T_1	H → L	52%				
		H−1 → L+1	48%	$\pi \rightarrow \pi^*$	2.66/465	0.00	IL/LMCT
	S_1	H → L	62%				
		H → L+1	36%	$\pi \rightarrow \pi^*$	3.34/371	0.01	IL/LMCT
$[Zn(PIm)_2]$	S_7	H−1 → L+2	45%				
(**3**)		H → L+4	41%	$\pi \rightarrow \pi^*$	4.10/302	0.31	IL/LMCT
	T_1	H → L	52%				
		H−1 → L+1	50%	$\pi \rightarrow \pi^*$	2.54/487	0.00	IL/LMCT
	S_1	H → L	60%				
		H−1 → L+1	39%	$\pi \rightarrow \pi^*$	3.22/386	0.02	LLCT/LMCT
$[Zn(PIm)_2(H_2O)]_2$	S_{20}	H−1 → L+2	44%				
(**7**)		H → L+3	43%	$\pi \rightarrow \pi^*$	4.00/310	0.34	IL/LMCT
	T_1	H → L	20%				
		H−3 → L	38%	$\pi \rightarrow \pi^*$	2.76/448	0.00	IL/LMCT
		H−2 → L+1	40%				

* H, HOMO; L, LUMO.

The $S_0 \rightarrow S_1$ and $S_0 \rightarrow T_1$ transition in both Zn systems is due primarily to the excitation of one electron from the HOMO to the LUMO; however, the nature of transition based on detailed consideration of molecular orbitals is different. To determine the characteristics of these transitions, the changes of electron-density distribution between the S_0 and S_1/T_1 state are calculated (shown in Fig. 4). It can be seen that the lowest singlet and triplet energy excitation of $[Zn(PIm)_2]$ (**3**) is attributed to intraligand electron transfer (IL) from imidazole ring to pyridyl ring, which closely resemble those of Cd pyridylimidazole systems (**2** and **4**), while in the case of $[Zn(PIm)_2(H_2O)]_2$ (**7**), charge transfer from one PIm ligand (B) to another PIm ligand (A) during $S_0 \rightarrow S_1$ excitation (LLCT) and localized intraligand charge transfer (within A) is observed in $S_0 \rightarrow T_1$ excitation.

The detailed characteristics of the intense transition in Zn pyridylimidazoles are revealed by Figure 4 and Table V. The absorption maximum in $[Zn(PIm)_2]$ (**3**) is due to an $S_0 \rightarrow S_7$ transition, which occurs presumably from imidazole ring to pyridyl ring delocalized on both PIm ligands (A and B). While the absorption peak in $[Zn(PIm)_2(H_2O)]_2$ (**7**) derived from $S_0 \rightarrow S_{20}$, corresponds to electron transfer localized on the single PIm ligand (B) (shown in Fig. 4). Such different transition patterns from monomer **3** to dimer **7** indicate the remarkable influence of axially coordinate water on spectral properties of the Zn pyridylimidazole complex.

Summary

In this work, a first-principles density functional method was employed to study the geometric and electronic structures of Zn(II), Cd(II) pyridyl imidazole complexes. The structural stability of model systems has been investigated in terms of the interaction of coordinated water with the center metal. The calculation results explain rationally that the experimental existence of the penta-coordinated Zn–water complexes with deprotonated pyridylimidazole can be ascribed to the effect of polariza-

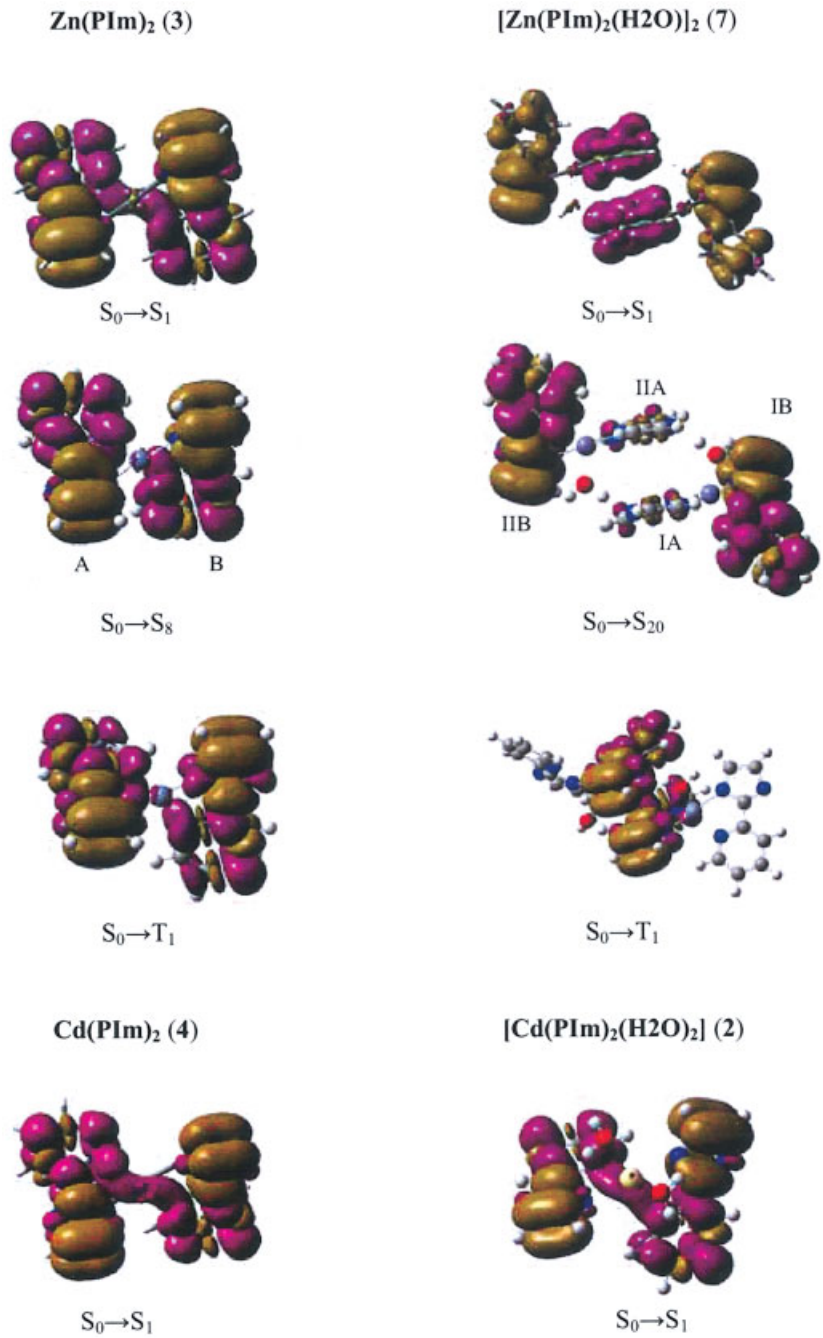

FIGURE 4. Change of electron density distribution upon the $S_0 \rightarrow S_n$ (T_1) electronic transition of Zn, Cd pyridylimidazole complexes. Yellow and violet colors correspond to a decrease and increase of electron density, respectively. [Color figure can be viewed in the online issue, which is available at www.interscience.wiley.com.]

tion from an intermolecular hydrogen bond. Such axially coordinated water in the Zn pyridylimidazole complex has a great impact on its spectral properties, while coordinated water in the Cd–pyridylimidazole complex has little effect on its photophysical properties. We hope our calculation results will enhance the understanding of the photophysical properties of the Zn, Cd–pyridylimidazole complexes and assist in the application of such complexes in the future.

ACKNOWLEDGMENT

The author gratefully thanks the National Science Foundation of China (No. 20373009 and 20162005) and the Youth Science Foundation of Northeast Normal University (111494018) for financial support.

Supporting Information Available

Materials are available free of charge via the Internet at http://www3.interscience.wiley.com, which include Illustration of $Cd(PBIm)_2$ and $Zn(PBIm)_2$, Figure of crystal packing for $Zn(PBIm)_2$ and experimental absorption spectra of $Cd(PBIm)_2$.

References

1. Holm, R. H.; Kennepohl, P.; Solomon, E. I. Chem Rev 1996, 96, 2239.
2. Toth, A.; Floriani, C.; Chiesi-Villa, A.; Guastini, C. Inorg Chem 1987, 26, 3897.
3. Rajan, R.; Rajaram, R.; Nair, B. U.; Ramasami, T.; Mandal, S. K. J Chem Soc Dalton Trans 1996, 9, 2019.
4. Cardwell, T. J.; Edwards, A. J.; Hartshorn, R. M.; Holmes, R. J.; McFadyen, W. D. Aust J Chem 1997, 50, 1009.
5. Bian, Z. Q.; Wang, K. Z.; Jin, L. P. Polyhedron 2002, 21, 313.
6. Shi, J.; Chen, C. H.; Klubek, K. P. US Patent Application 1997, 75, 897.
7. Huang, L.; Wang, K. Z.; Huang, C. H.; Li, F. Y.; Huang, Y. Y. J Mater Chem 2001, 11, 790.
8. Yue, S. M.; Chen, S. C.; Su, Z. M.; Ma, J. F.; Chu, B.; Kan, Y. H. Polyhedron (accepted).
9. Cotton, F. A.; Wilkinson, G. Advanced Inorganic Chemistry; Interscience: New York, 1980.
10. Morassi, R.; Bertini, I.; Sacconi, L. Coord Chem Rev 1973, 11, 343.
11. Kerr, M. C.; Preston, H. S.; Ammon, H. L.; Huheey, J. E.; Stewart, J. M. J Coord Chem 1981, 11, 111.
12. Bhattacharyya, S.; Kumar, S. B.; Dutta, S. K.; Tiekink, E. R. T.; Chaudhury, M. Inorg Chem 1996, 35, 1967.
13. Liu, S. F.; Wu, Q. G.; Wang, S. J Am Chem Soc 2000, 122, 3671.
14. Beeby, A.; Clarkson, L. M.; Dickins, R. S.; Faulkner, S.; Parker, D.; Royle, L.; de Sousa, A. S.; Williams, J. A. G.; Woods, M. J. Chem Soc Perkin Trans 1999, 2, 493.
15. Yanagida, S.; Hasegawa, Y.; Murakoshi, K.; Wada, Y.; Nakashima, N.; Yamanaka, T. Coord Chem Rev 1998, 171, 461.
16. Frisch, M. J.; Trucks, G. W.; Schlegel, H. B.; Scuseria, G. E.; Robb, M. A.; Cheeseman, J. R.; Zakrzewski, V. G.; Montgomery, J. A., Jr.; Stratmann, R. E.; Burant, J. C.; Dapprich, S.; Millam, J. M.; Daniels, A. D.; Kudin, K. N.; Strain, M. C.; Farkas, O.; Tomasi, J.; Barone, V.; Cossi, M.; Cammi, R.; Mennucci, B.; Pomelli, C.; Adamo, C.; Clifford, S.; Ochterski, J.; Petersson, G. A.; Ayala, P. Y.; Cui, Q.; Morokuma, K.; Malick, D. K.; Rabuck, A. D.; Raghavachari, K.; Foresman, J. B.; Cioslowski, J.; Ortiz, J. V.; Stefanov, B. B.; Liu, G.; Liashenko, A.; Piskorz, P.; Komaromi, I.; Gomperts, R.; Martin, R. L.; Fox, D. J.; Keith, T.; Al-Laham, M. A.; Peng, C. Y.; Nanayakkara, A.; Gonzalez, C.; Challacombe, M.; Gill, P. M. W.; Johnson, B.; Chen, W.; Wong, M. W.; Andres, J. L.; Gonzalez, C.; Head-Gordon, M.; Replogle, E. S.; Pople, J. A. Gaussian 03; Revision A.1; Gaussian: Pittsburgh, PA, 2003.
17. Becke, A. D. J Chem Phys 1993, 98, 5648.
18. Lee, C.; Yang, W.; Parr, R. G. Phys Rev B 1988, 37, 785.
19. Ziegler, T. Chem Rev 1991, 91, 651.
20. Niu, S.; Hall, M. B. Chem Rev 2000, 100, 353.
21. Conner, D.; Jayaprakash, K. N.; Cundari, T. R.; Gunnoe, T. B. Organometallics 2004, 23, 2724.
22. Iron, M. A.; Martin, J. M. L.; Van der Boom, M. E. J Am Chem Soc 2003, 125, 11702.
23. Hariharan, P. C.; Pople, J. A. Theor Chim Acta 1973, 28, 213.
24. Hay, P. J.; Wadt, W. R. J Chem Phys 1985, 82, 270.
25. Ransil, B. J. J Chem Phys 1961, 34, 2109.
26. Boys, S. F.; Bernardi, F. Mol Phys 1970, 19, 553.
27. Casida, M. E.; Jamorski, C.; Casida, K. C.; Salahub, D. R. J Chem Phys 1998, 108, 4439.
28. Casida, M. E. Accurate Description of Low-Lying Molecular States and Potential Energy Surfaces; Hoffmann, M. R., Dyall, K. G., Eds.; American Chemical Society: Washington, DC, 2002; p 199.
29. Daniel, C. Coord Chem Rev 2003, 238/239, 143.
30. Adamo, C.; Barone, V. Theor Chem Acc 2000, 105, 169.
31. Boulet, P.; Chermett, H.; Daul, C.; Gilardoni, F.; Rogemond, F.; Weber, J.; Zuber, G. J. Phys Chem A 2001, 105, 885.
32. Stoyanov, S. R.; Villegas, J. M.; Rillema, D. P. Inorg Chem 2003, 42, 7852.
33. Charmant, J. P. H.; Fornie's, J.; Go'mez, J.; Lalinde, E.; Merino, R. I.; Moreno, M. T.; Orpen, A. G. Organometallics 2003, 22, 652.
34. Halls, M. D.; Schlegel, H. B. Chem Mater 2001, 13, 2632.
35. Martin, R. L.; Kress, J. D.; Campbell, I. H. Phys Rev B 2000, 61, 15804.
36. Han, Y. K.; Lee, S. U. Chem Phys Lett 2002, 366, 9.
37. Hoskins, B. F.; Whillans, F. D. Coord Chem Rev 1972–1973, 9, 365.
38. Åkesson, R.; Pettersson, L. G. M.; Siegbahn, P. E. M. J Phys Chem 1992, 96, 10773.
39. Pearson, R. G. J Am Chem Soc 1963, 85, 3533.
40. Pearson, R. G. Coord Chem Rev 1990, 100, 403.
41. Badley, R. Fluorescence Spectroscopy; Plenum: New York, 1983.